





RESEARCH ARTICLE

Prediction for oxaliplatin-induced liver injury using patient-derived liver organoids

Kumiko Tatsumi^{1,2}  | Hiroshi Wada³ | Shinichiro Hasegawa³ | Kei Asukai³ | Shigenori Nagata⁴ | Tomoya Ekawa¹ | Takashi Akazawa¹  | Yu Mizote¹  | Shintaro Okumura²  | Ryosuke Okamura² | Masayuki Ohue³ | Kazutaka Obama² | Hideaki Tahara^{1,5}

¹Department of Cancer Drug Discovery and Development, Research Center, Osaka International Cancer Institute, Osaka, Japan

²Department of Surgery, Graduate School of Medicine, Kyoto University, Kyoto, Japan

³Department of Gastroenterological Surgery, Osaka International Cancer Institute, Osaka, Japan

⁴Department of Diagnostic Pathology and Cytology, Osaka International Cancer Institute, Osaka, Japan

⁵Project Division of Cancer Biomolecular Therapy, The Institute of Medical Science, The University of Tokyo, Tokyo, Japan

Correspondence

Shintaro Okumura, Department of Surgery, Graduate School of Medicine, Kyoto University, 54 Shogoin-Kawahara-cho, Sakyo-ku, Kyoto 606-8507, Japan.

Email: sokumura@kuhp.kyoto-u.ac.jp

Funding information

Osaka International Cancer Institute; Japan Agency for Medical Research and Development, Grant/Award Number: 22ak0101187h0101

Abstract

Background: Liver injury associated with oxaliplatin (L-OHP)-based chemotherapy can significantly impact the treatment outcomes of patients with colorectal cancer liver metastases, especially when combined with surgery. To date, no definitive biomarker that can predict the risk of liver injury has been identified. This study aimed to investigate whether organoids can be used as tools to predict the risk of liver injury.

Methods: We examined the relationship between the clinical signs of L-OHP-induced liver injury and the responses of patient-derived liver organoids *in vitro*. Organoids were established from noncancerous liver tissues obtained from 10 patients who underwent L-OHP-based chemotherapy and hepatectomy for colorectal cancer.

Results: Organoids cultured in a galactose differentiation medium, which can activate the mitochondria of organoids, showed sensitivity to L-OHP cytotoxicity, which was significantly related to clinical liver toxicity induced by L-OHP treatment. Organoids from patients who presented with a high-grade liver injury to the L-OHP regimen showed an obvious increase in mitochondrial superoxide levels and a significant decrease in mitochondrial membrane potential with L-OHP exposure. L-OHP-induced mitochondrial oxidative stress was not observed in the organoids from patients with low-grade liver injury.

Conclusions: These results suggested that L-OHP-induced liver injury may be caused by mitochondrial oxidative damage. Furthermore, patient-derived liver organoids may be used to assess susceptibility to L-OHP-induced liver injury in individual patients.

KEYWORDS

liver injury, organoids, oxaliplatin, oxidative stress, sinusoidal obstruction syndrome

1 | INTRODUCTION

Oxaliplatin (L-OHP)-based regimens are the current standard chemotherapy for metastatic colorectal cancer. Pharmacotherapy with cancer drugs, including L-OHP, prolongs the overall survival of patients diagnosed with unresectable advanced metastatic colorectal cancer and may also allow curative resection for metastatic lesions.^{1,2} For resectable liver metastases, L-OHP may be administered as perioperative chemotherapy for patients at high risk of recurrence or incomplete resection. Despite its therapeutic efficacy, liver injury associated with an L-OHP-based regimen may lead to morbidity or liver failure following liver resection.^{3,4} Furthermore, precautions for such injury often lead to compromised dosing with an increased risk of early recurrence.⁵ Thus, regimens have to be carefully determined and administered to each patient according to the individual risk of liver injury. However, the management of liver injury has been problematic because of the lack of accurate and reliable biomarkers for predicting the risk of liver injury.

Several biomarkers have been reported to be useful for predicting chemotherapy-associated side effects in patients with colorectal cancer. Laboratory testing to determine the *UGT1A1* polymorphism helps in predicting the severe side effects such as severe leukopenia or diarrhea by irinotecan.^{6–8} The European Medicines Agency recommends the test for dihydropyrimidine dehydrogenase enzyme deficiency, which is related to serious side effects, before starting cancer treatment with the 5-fluorouracil series.^{9,10} For L-OHP, Glutathione *S*-transferase M1 (*GSTM1*)-null genotype is reported as an independent risk factor for liver injury caused by sinusoidal obstruction syndrome (SOS) in patients with metastatic colorectal cancer.¹¹ However, to date, the accuracy of this biomarker remains debated and thus has not been applied in clinical practice. Therefore, new strategies are needed to identify biomarkers, particularly for L-OHP-induced liver injury.

Recently, patient-derived cancer organoids have been considered useful tools to answer clinical questions.¹² Results of drug sensitivity tests using patient-derived organoids have been shown to have a significant correlation with the therapeutic outcomes of patients in some models, including L-OHP,^{13–15} suggesting that patient-derived cancer organoids may be useful in predicting the therapeutic effectiveness of cancer drugs in individual patients. Thus, if patient-derived liver organoids could also be used to predict L-OHP-induced liver injury in treated patients, the risks and benefits of chemotherapy could be assessed before initiating treatment.

Huch et al. reported that liver stem cell-derived organoids (liver organoids) can be effectively established from a limited amount of liver tissue in the short term. They

demonstrated the ability to expand these organoids over an extended period while maintaining genetic stability. Additionally, the liver organoids were successfully induced to undergo functional maturation.¹⁶ Taking advantage of these characteristics, liver organoids have emerged as valuable tools in the study of hereditary liver diseases, such as α -1 antitrypsin deficiency.¹⁷ Nevertheless, the potential utility of patient-derived liver organoids as predictive models for assessing liver injury caused by chemotherapeutic drugs, including L-OHP, in actual patients remains largely unexplored.¹⁸ Liver injury linked to L-OHP-based regimens does not manifest uniformly among all patients but rather in certain individuals with varying degrees of severity.^{19,20} This observation implies the presence of individual variations in response to L-OHP. Therefore, it would be beneficial if patient-derived liver organoids could be used to predict liver injury caused by L-OHP. In this study, we found that liver organoids established using our method from non-cancerous liver tissue of patients could be used to predict L-OHP-induced liver injury.

2 | MATERIALS AND METHODS

2.1 | Clinical information and specimens

In this study, we enrolled 10 patients who were treated with L-OHP-based neoadjuvant chemotherapy and hepatectomy for colorectal cancer liver metastasis at the Osaka International Cancer Institute between April 2019 and February 2020. Clinical information and non-cancerous liver tissue samples were collected from subjects who provided written informed consent. This study was approved by the ethics committee of Osaka International Cancer Institute (IRB protocol number 18231). The tissue samples were stored in ice-cold Dulbecco's Modified Eagle's medium/nutrient Mixture F12 (DMEM/F12; Gibco) until processing.

2.2 | Assessment of liver injury associated with L-OHP-based chemotherapy

Liver injury associated with L-OHP-based chemotherapy was assessed based on the serum aspartate transaminase (AST), alanine transaminase (ALT), total bilirubin (T-Bil), and alkaline phosphatase (ALP). The severity of the liver injury was estimated using the Common Terminology Criteria for Adverse Events (CTCAE) v5.0.²¹ The patients were divided into two groups: the high-grade group, characterized by a grade 1 or higher elevation in both AST and ALT, and the low-grade group.^{4,22} The L-OHP-related

injury was defined by changes in the spleen size²³ and histopathological findings.²⁴ Details are provided in Appendix S1.

2.3 | Liver organoid culture

Liver organoids were established and differentiated into hepatocytes, as described in Appendix S1. Differentiated liver organoids were cultured in a glucose-based hepatocyte differentiation medium (standard differentiation medium) or galactose-based hepatocyte differentiation medium (galactose differentiation medium) for in vitro assays. *N*-acetyl-L-cysteine (NAC) was absent during L-OHP treatment.

2.4 | Lactate dehydrogenase (LDH) leakage assay

Cytotoxicity was assessed by measuring LDH released from the cytoplasm into the culture medium upon loss of cytoplasmic membrane integrity.²⁵ Cells were seeded at a density of 1500 cells into a 96-well plate in triplicate, cultured in expansion medium supplemented with 25 ng/mL human BMP-7 (R&D Systems, 354-BP-010) for 3–5 days, and then cultured with differentiation medium until the LDH leakage assay. After hepatocyte differentiation, the organoids were cultured in a differentiation medium (NAC-free) containing rotenone (TCl, R0090) or L-OHP (TCl, O0372). For the rotenone treatment, the supernatant was collected 24 h later. For the L-OHP treatment, the supernatant was collected and replaced with a fresh drug-containing medium every 24 h for up to 72 h. The L-OHP doses were set from the maximum plasma concentration (C_{\max}) during clinical administration to doses of up to four times higher than C_{\max} . LDH activity was measured using an LDH Cytotoxicity Assay Kit (Nacalai Tesque) according to the manufacturer's protocol. Absorbance was measured at 490 nm using a Multimode Microplate Reader Infinite M200 Plex (Tecan). LDH release and the cytotoxicity index were calculated according to the following formula²⁶:

$$\text{LDH release (\%)} = \frac{\text{experimental release}}{\text{maximum release}} \times 100$$

$$\text{Cytotoxicity index} = \frac{(\text{experimental release} - \text{spontaneous release})}{(\text{maximum release} - \text{spontaneous release})} \times 100$$

Spontaneous release represents LDH released from untreated cells, and maximum release represents LDH released from cells treated with lysis buffer. Additional

information for in vitro experiments is described in Appendix S1.

2.5 | Statistical analyses

Statistical differences for single comparisons were evaluated using a two-sided Welch's *t*-test or the non-parametric Mann–Whitney *U* test. Statistical differences for multiple comparisons were evaluated using a one-way ANOVA with Dunnett's test. All statistical tests were performed using GraphPad PRISM 8. $p < 0.05$ was considered statistically significant.

3 | RESULTS

3.1 | Assessment of liver injury in patients receiving L-OHP-based chemotherapy

To investigate individual differences in their susceptibility to L-OHP-induced liver injury, 10 patients who underwent liver resection after receiving L-OHP chemotherapy were recruited for analysis. The clinical information of the 10 patients is presented in Table 1. Among the 10 patients, three patients (LM24, LM14, and LM10) who developed grade 1 or higher elevation of both AST and ALT in the blood test data were classified into the high-grade liver injury group. The remaining seven patients (LM7, LM19, LM1, LM11, LM15, LM16, and LM23) who developed grade 1 elevation in either AST or ALT or no elevation in both AST and ALT levels were classified into the low-grade liver injury group.

We examined the increase in spleen size which is a clinical characteristic of L-OHP-induced hepatotoxicity.²³ An increase in spleen size following L-OHP-based chemotherapy was observed in the high-grade group, while such an increase was not prominently observed in the low-grade group (Table 1). Furthermore, a histopathological examination was performed to estimate the presence of L-OHP-related liver injury. In the liver tissues of three patients in the high-grade group, sinusoidal dilation, centrilobular/venular fibrosis (except for LM14), nodular transformation, and hepatocellular damage were observed (Figure 1A,B,C, Table S1). These pathological findings are compatible with the characteristics of the liver with L-OHP-induced hepatotoxicity.²⁴ In contrast, in the liver tissues of seven patients in the low-grade group, histological changes were relatively mild (Figure S1, Table S1). Thus, the histopathological changes observed in the liver tissues were consistent with the grade of liver injury in the blood test data (Table 1).

TABLE 1 Clinical information of subjects including chemotherapy regimens and liver injury.

Liver Injury	Patient I.D.	Age	Sex	L-OHP based chemotherapy		CTCAE grade				Spleen size (post/pre)
				Regimen	Cycles	AST	ALT	T-Bil	ALP	
High	LM24	49	Male	XELOX	8	3	3	1	2	1.6
High	LM14	77	Female	mFOLFOX6	6	1	1	–	–	1.3
High	LM10	37	Male	XELOX	5	1	1	–	–	2.3
Low	LM7	61	Male	XELOX	3	1	–	–	–	0.9
Low	LM19	58	Male	FOLFOXIRI	10	–	1	–	1	1.0
Low	LM1	67	Male	mFOLFOX6	8	–	–	–	–	1.0
Low	LM11	38	Female	mFOLFOX6	5	–	–	–	–	0.9
Low	LM15	58	Male	XELOX	8	–	–	–	–	1.0
Low	LM16	70	Female	XELOX	4	–	–	–	–	1.1
Low	LM23	70	Male	mFOLFOX6	8	–	–	–	–	1.0

Note: Spleen size (post/pre) = spleen volume after chemotherapy/spleen volume before chemotherapy. Spleen volume was calculated by multiplying the length, thickness, and width.

Abbreviations: ALP, alkaline phosphatase; ALT, alanine aminotransferase; AST, aspartate aminotransferase; FOLFOXIRI, leucovorin, 5-fluorouracil, irinotecan, and L-OHP; T-Bil, total bilirubin; XELOX, capecitabine and L-OHP; mFOLFOX6, leucovorin, 5-fluorouracil, and L-OHP.

3.2 | Liver organoids cultured in standard differentiation medium do not show cytotoxic reactions with L-OHP treatment

In all 10 patients, organoids were successfully established from non-cancerous liver tissues within 2 weeks. Organoids cultured in an expansion medium consisted of a single-layered epithelium, whereas those cultured in a differentiation medium changed to a stratified polygonal epithelium (Figure S2A,B). Compared to the organoids in the expansion medium, the organoids in the differentiation medium expressed the adult stem cell marker (*LGR5*) at a lower level and the mature hepatocyte markers (*HNF4A*, *ALB*, and *CYP3A4*) at higher levels (Figure S2C). These characteristics were similar to those reported for liver organoids by Huch et al.¹⁶

To develop an in vitro assay to predict the likelihood of liver injury related to L-OHP in patients, we examined the cytotoxic effects of L-OHP on liver organoids cultured in a standard differentiation medium. Even with repeated doses of 40 μ M L-OHP, which is a quadruple dose of C_{\max} during clinical administration, the average levels of LDH release in the high- and low-grade groups were $6.9 \pm 1.9\%$ and $6.5 \pm 3.2\%$, respectively (Figure S3A). Furthermore, the levels of L-OHP-induced cytotoxicity were not significantly different between the two groups at any concentration of L-OHP (Figure S3B). These results suggest that in vitro assays under these culture conditions may not be sensitive enough to predict the likelihood of liver injury related to L-OHP in these patients.

It has been reported that L-OHP leads to the generation of reactive oxygen species (ROS) from the mitochondria and can result in liver injury.^{27–29} Therefore, it was considered that the cytotoxic effects of L-OHP cannot be fully observed in cells with insufficient mitochondrial activity. Thus, we performed a JC-1 assay to detect mitochondrial membrane potential as a parameter of mitochondrial condition. Red fluorescence represents JC-1 aggregates appearing at high membrane potentials, indicating healthy mitochondria. As shown in Figures S3C and S4, liver organoids from all 10 patients showed green fluorescence (JC-1 monomers), whereas red fluorescence (JC-1 aggregates) was not observed. These results suggest that the mitochondria were inactive under these culture conditions. Therefore, the cytotoxic effects of L-OHP could not be accurately estimated using the assay conditions described above.

3.3 | Liver organoids cultured in galactose differentiation medium show sensitivity to L-OHP cytotoxicity correlating with the grade of L-OHP liver injury in patients

In a previous study, it was shown that isolated primary mature hepatocytes switch energy production from mitochondrial oxidative phosphorylation to glycolysis in a high glucose medium.³⁰ Given that the standard differentiation medium contains high glucose, liver organoids in such conditions may also rely on glycolysis as their major source of energy production. We hypothesized that

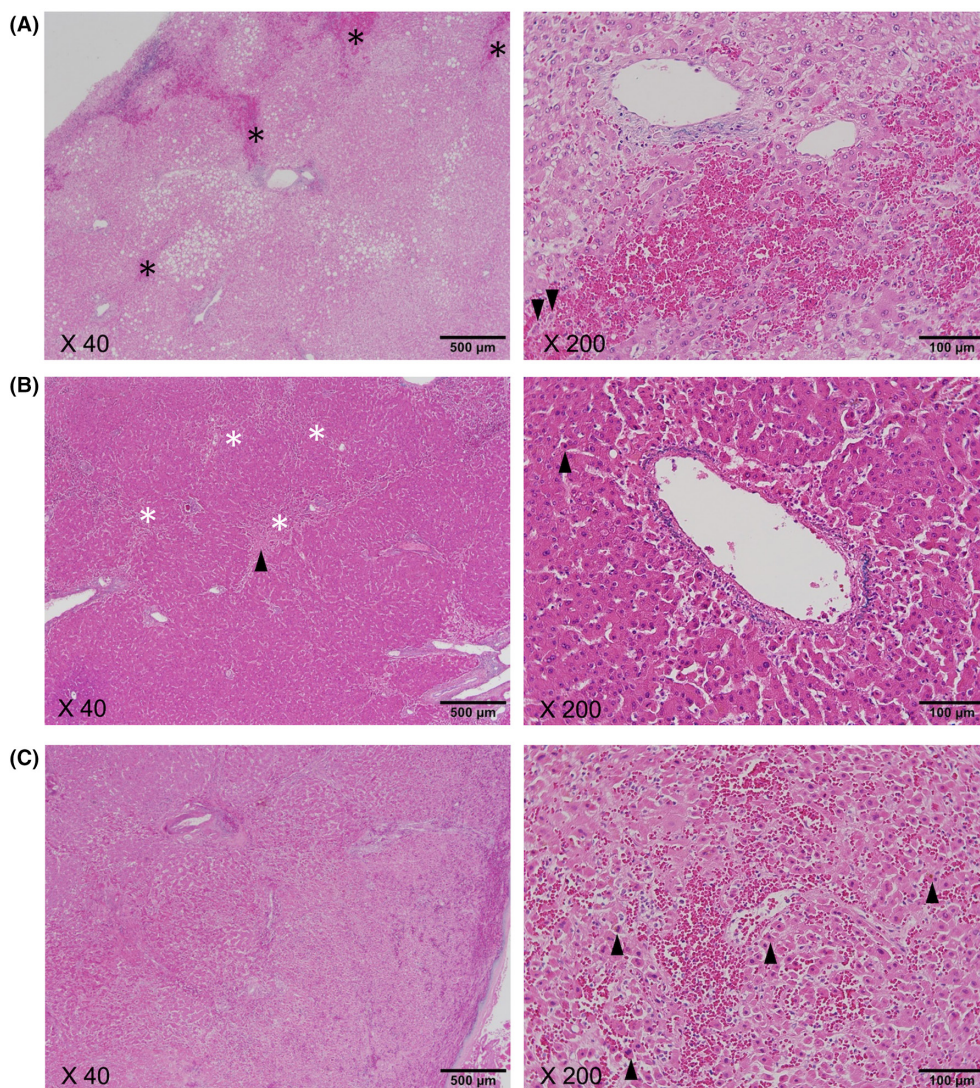


FIGURE 1 Histology of liver tissues in the high-grade liver injury group. (A–C) Representative Victoria-Blue (VB)-H&E staining images of non-cancerous liver tissues treated with L-OHP-based chemotherapy. Low- and high-power fields are shown in the left and right panels, respectively. (A) Panel of LM10. Sinusoidal congestion (black asterisks) was observed (left panel). Moderate sinusoidal dilatation around the central vein, hepatocyte atrophy, hepatocyte degeneration (arrowheads), and congestion were observed (right panel). (B) Panel of LM24. Sinusoidal dilatation and hepatocyte atrophy (white asterisks), and hepatocyte degeneration (arrowhead) were observed (left panel). Mild sinusoidal dilatation around the central vein and hepatocyte degeneration (arrowhead) were observed (right panel). (C) Panel of LM14. Lobular lesions with sinusoidal dilatation are observed (left panel). Moderate to severe sinusoidal dilatation around the central vein, disordered hepatocyte arrangement, and hepatocyte degeneration (arrowheads) were observed (right panel).

this might be the reason why mitochondria-related toxicity was not observed, as described above. HepG2 cells, which are widely used for mitochondrial toxicity studies, grown in the presence of galactose instead of glucose, are reportedly forced to shift most of their energy production to mitochondrial oxidative phosphorylation and exhibit sensitivity to mitochondrial toxins.³¹ In this study, we investigated whether the medium in which glucose was replaced with galactose could be applied to liver organoids and used for cytotoxicity assays.

Among the 10 patients, LM24 developed the highest elevation in AST, ALT, T-Bil, and ALP, whereas LM1

developed no elevation in these blood test items associated with liver damage (Table 1). LM24 and LM1 were used as representatives of the high- and low-grade groups, respectively. LM24 and LM1 cultured in galactose differentiation medium maintained similar shapes and produced similar amounts of ATP as those cultured in standard differentiation medium (Figure 2A,B). Unlike in the standard differentiation medium, the mitochondria of the organoids were active in the galactose differentiation medium (Figure S3C, S4, 2C). Since there was no apparent difference in the basal mitochondrial activity between the high- and low-grade groups, we proceeded with further analysis.

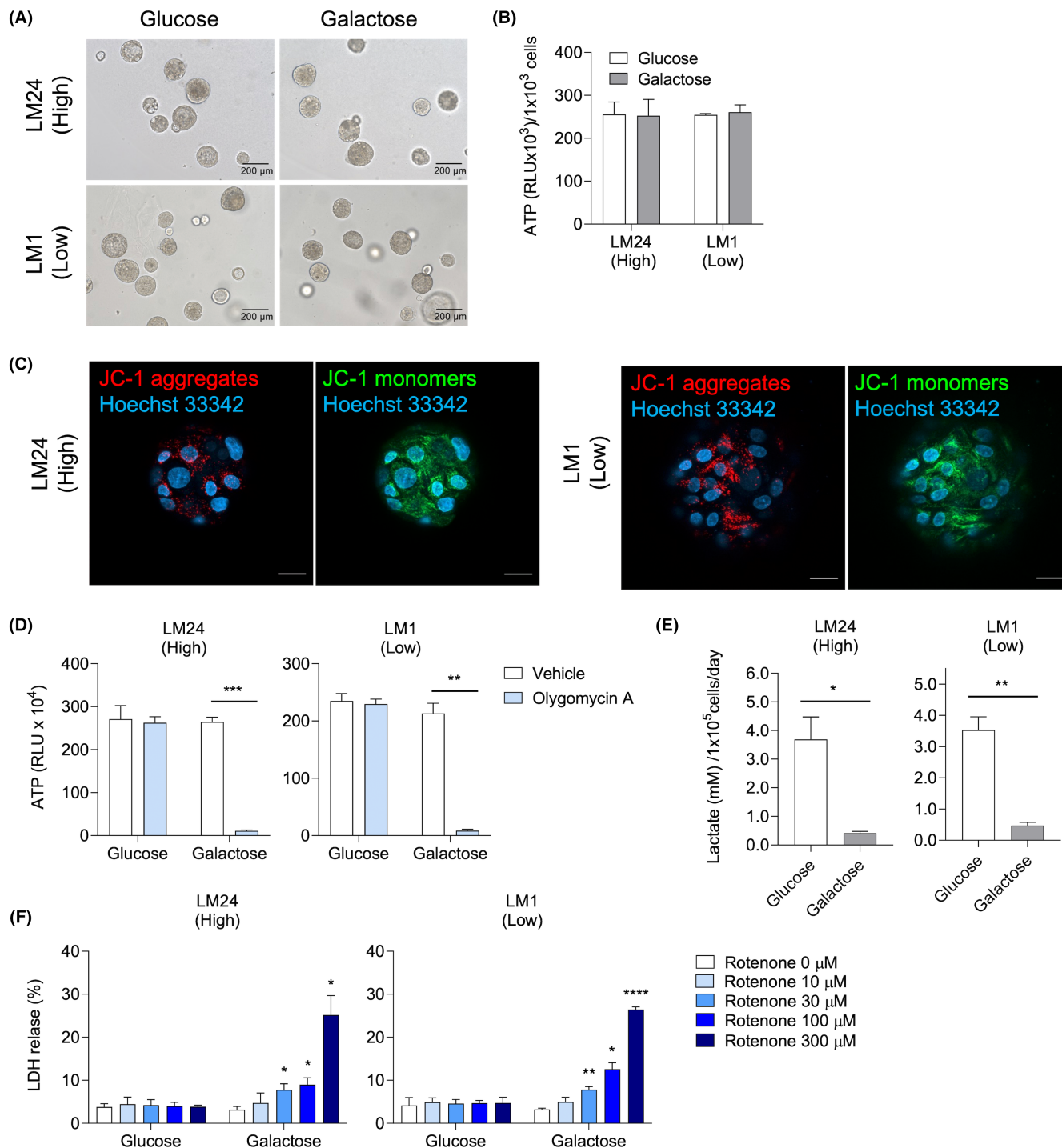


FIGURE 2 Differences in mitochondrial activity of liver organoids between standard differentiation medium and galactose differentiation medium. (A–F) Liver organoids of LM24 (high-grade group) and LM1 (low-grade group) were cultured in standard (glucose) or galactose differentiation medium for 8–11 days. (A) Representative brightfield images of liver organoids. (B) Cell viability was evaluated by measuring intracellular ATP levels. (C) Mitochondrial condition was evaluated with a JC-1 probe. Representative images of JC-1-stained liver organoids are shown. Red, JC-1 aggregates; green, JC-1 monomers; blue, Hoechst 33342 (nuclei). Scale bar, 20 μ m. (D) Intracellular ATP levels of liver organoids cultured with vehicle (0.3% DMSO) or 5 μ M oligomycin A for 2 h. (E) The amount of lactate in the medium after 24 h culture. (F) LDH release from liver organoids treated with rotenone at the indicated concentrations. These assays were performed in duplicate and representative data were shown. Bars indicate mean \pm SD. Statistical significance was determined with a two-sided Welch's *t*-test (D, E) or ANOVA followed by Dunnett's test (compared with 0 μ M of rotenone) (F). **p* < 0.05, ***p* < 0.01, ****p* < 0.001, *****p* < 0.0001.

Next, we examined the dependence of liver organoids on mitochondrial oxidative phosphorylation during energy production. Intracellular ATP levels were measured in the presence of oligomycin A, an inhibitor of mitochondrial ATP synthase.³² In the standard differentiation medium, oligomycin A had no effect, whereas oligomycin A resulted in a dramatic decrease of ATP content in the galactose differentiation medium (Figure 2D). In addition, LM24 and LM1 organoids cultured in galactose differentiation medium produced significantly less lactic acid, a glycolysis metabolite, than those cultured in standard differentiation medium (Figure 2E). These results strongly suggest that the galactose differentiation medium enables energy production in liver organoids through mitochondrial oxidative phosphorylation instead of glycolysis. Furthermore, to confirm the sensitivity to mitochondrial toxins, we treated LM24 and LM1 organoids with rotenone. Rotenone is an inhibitor of mitochondrial electron transport chain complex I and leads to the restriction of ATP synthesis.³³ Both LM24 and LM1 exhibited no significant increase in LDH leakage when cultured in the standard differentiation medium. However, when exposed to a galactose differentiation medium, both organoids demonstrated a concentration-dependent elevation

in LDH leakage (Figure 2F). These results indicated that mitochondrial injury-induced cytotoxicity could be examined if the galactose differentiation medium was used for the culture of liver organoids.

Liver organoids from each patient were cultured in a galactose differentiation medium and tested for L-OHP cytotoxicity. With a repeated maximum dose of 40 μ M L-OHP, LDH release levels for the high- and low-grade groups were $13.4 \pm 2.1\%$ and $6.5 \pm 2.3\%$, respectively (Figure 3A). Organoids in the high-grade group showed significantly higher levels of LDH release, which were not observed in cultures in the standard differentiation medium (Figure S3A, 3A). Moreover, the organoids in the high-grade group showed significantly higher cytotoxicity indices after L-OHP treatment than those in the low-grade group (Figure 3B).

3.4 | L-OHP-induced liver toxicity is caused by mitochondrial oxidative damage

Mitochondrial conditions were evaluated using the JC-1 assay. The liver organoids showed a decrease in red fluorescence with treatment of CCCP, a mitochondrial oxidative

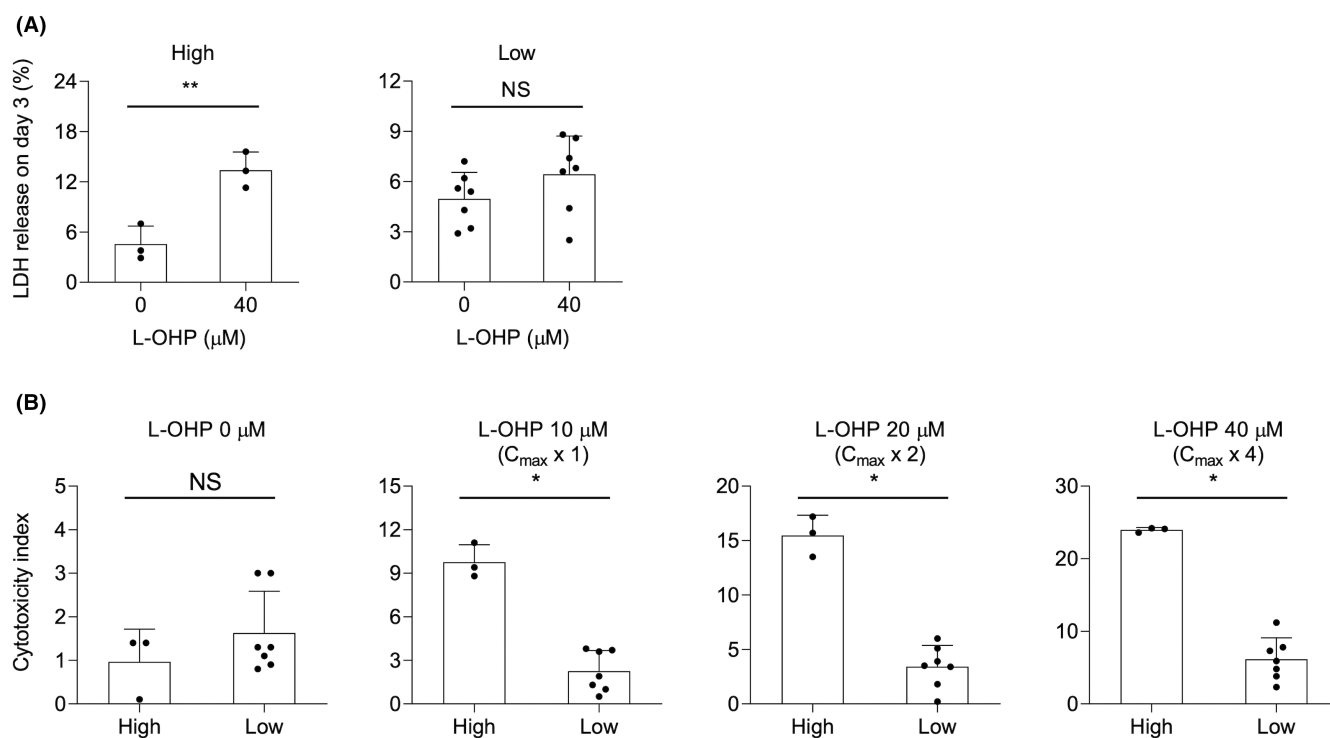


FIGURE 3 L-OHP-induced cytotoxicity in liver organoids cultured in galactose differentiation medium. (A and B) Liver organoids cultured for 5 days in standard differentiation medium followed by 3 days in galactose differentiation medium were subjected to repeated doses of L-OHP. (A) LDH release from liver organoids on day 3 of repeated doses of L-OHP. (B) Cytotoxicity index of liver organoids treated with repeated doses of L-OHP at the indicated concentrations for 72 h. Each dot indicates independent patients in the high- or low-grade groups. Bars indicate mean \pm SD. Statistical significance was determined with a two-sided Welch's *t*-test (A) or two-sided Mann-Whitney *U* test (B). **p* < 0.05, ***p* < 0.01. NS, Not Significant.

phosphorylation uncoupler, indicating that the JC-1 assay was working (Figure 4A). The liver organoids of the low-grade group showed no significant changes in the fluorescence intensity ratio (red [JC-1 aggregates]/green [JC-1 monomers]) with L-OHP treatment compared to vehicle treatment. However, liver organoids of the high-grade group showed a significant decrease in the fluorescence intensity ratio (Figure 4A,C). To investigate the generation of mitochondrial ROS by L-OHP treatment, mitochondrial superoxide ($O_2^{\bullet-}$) after 2 h of L-OHP treatment was examined using a mtSOX Deep Red probe emitting red fluorescence. In liver organoids from multiple patients, red fluorescence was significantly increased with L-OHP treatment compared to vehicle treatment, exhibiting spontaneous generation. Importantly, the high-grade group showed an obvious increase in red fluorescence compared with the low-grade group (Figure 4B,D). In the high-grade group, the decreased mitochondrial activity was consistent with increased superoxide generation. Moreover, within the high-grade group, there was an observed increase in the total intracellular glutathione (GSH) levels 24 h following L-OHP treatment. However, these levels subsequently decreased over time. LM1, which was used as a representative for the low-grade group, showed increasing GSH levels with the repeated administration of L-OHP when compared to the high-grade group (Figure 4E). GSH is a well-recognized direct antioxidant that is widely involved in the cellular removal of H_2O_2 and other hydroperoxides.^{34,35} When cells are under oxidative stress, GSH biosynthesis is promoted by free radicals.³⁶ Our results suggest that GSH is transiently biosynthetically increased by L-OHP treatment and then consumed. NAC acts as a direct and indirect antioxidant by upregulating antioxidant enzymes such as Mn-SOD, Cu/Zn-SOD, glutathione peroxidase (GSH-Px), and catalase (CAT), or by acting as a GSH precursor.^{35,37} Cytotoxicity was suppressed by the concomitant use of high-dose NAC (Figure 4F). Thus, L-OHP-induced cytotoxicity in the liver organoids may be attributed to mitochondrial oxidative damage.

Finally, to develop a simple and clinically applicable test method for the assessment of mitochondrial oxidative

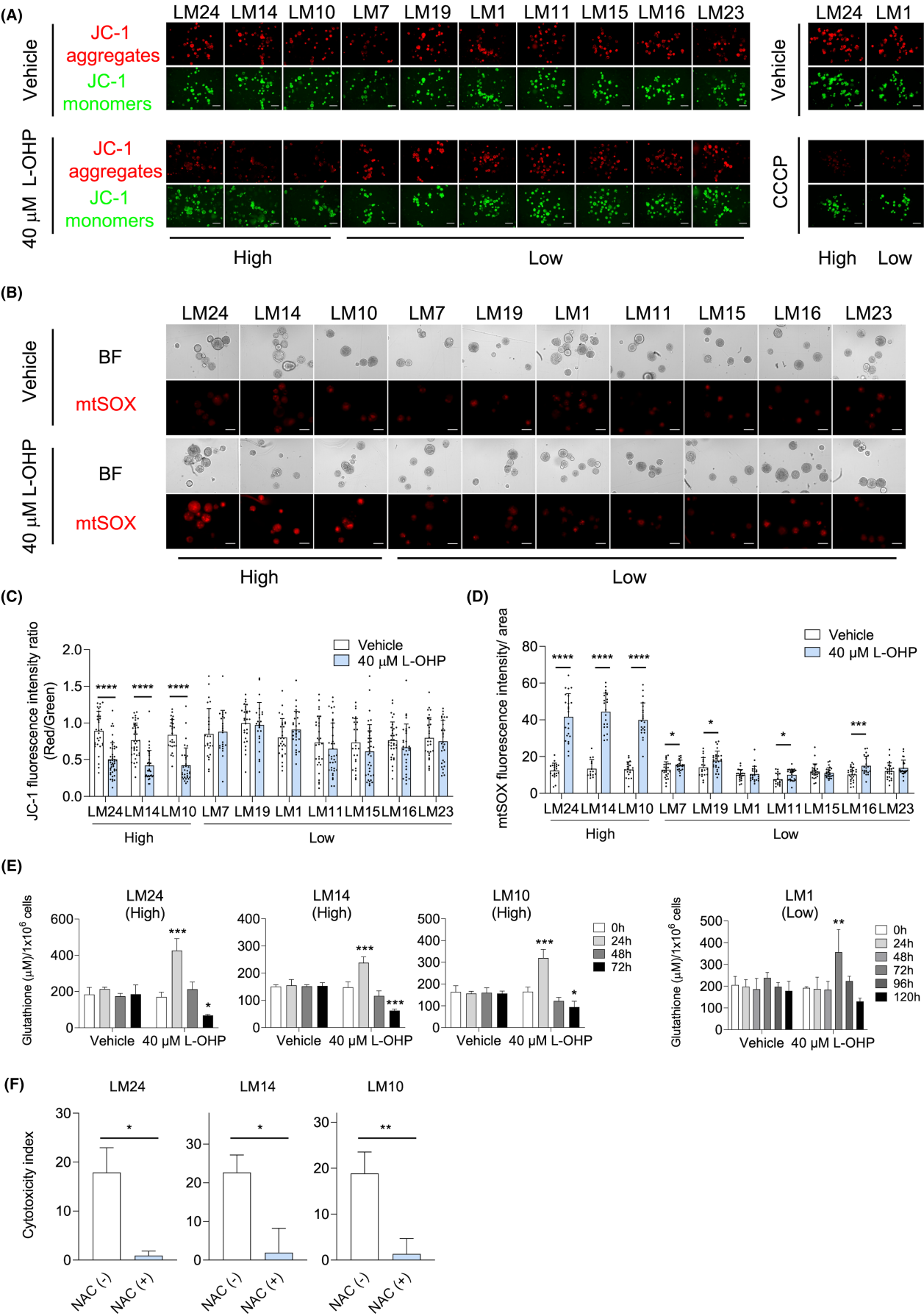
damage in patients, we examined the intracellular ATP levels in liver organoids cultured under different conditions. Liver organoids from each patient were cultured in standard or galactose differentiation media and treated with a single dose of L-OHP for 72 h. Intracellular ATP levels in organoids from the high-grade group showed significant differences between the two types of media in the range of 20–160 μ M L-OHP at multiple points. At an L-OHP concentration of 80 μ M, the liver organoids from the high-grade group showed significantly higher ATP ratios than those of liver organoids from the low-grade group (Figure 5A,B).

4 | DISCUSSION

While surgical resection of colorectal cancer liver metastasis can prolong survival time,³⁸ it is important to note that the recurrence of liver metastasis is a common occurrence, with rates ranging between 45% and 70%.^{39,40} In such situations, the majority of these patients are typically treated with chemotherapy.^{2,39} We have proposed an in vitro examination method to assess the susceptibility of L-OHP-induced liver injury using patient-derived liver organoids. This assessment could prove highly beneficial for selecting appropriate treatment options, such as chemotherapy with or without L-OHP or treatment prior to surgical resection in the event of recurrence. The advantage of this approach is that the assessment can be completed within approximately 1 month after liver resection. This timeframe allows for an ample window to assess the susceptibility of L-OHP-induced liver injury and devise a treatment strategy before recurrence is confirmed.

Multiple investigators have examined the usefulness of patient-derived liver organoids for evaluating drug potency in vitro. However, we found that the mitochondrial functions of liver organoids could not be fully examined if the liver organoids were cultured in commonly used maturation media. To improve this status, we developed an appropriate culture condition and examined the mechanism of L-OHP toxicity, which has been implicated in oxidative stress in mouse models.²⁸

FIGURE 4 L-OHP-induced mitochondrial oxidative stress in liver organoids in each patient. (A–F) Liver organoids cultured for 5 days in standard differentiation medium followed by 3 days in galactose differentiation medium were subjected to a single dose or repeated doses of L-OHP. (A) Mitochondrial condition was evaluated with a JC-1 probe after the repeated doses of L-OHP for 48 h or CCCP treatment for 1.5 h. Representative images of JC-1-stained liver organoids are shown. Red, JC-1 aggregates; green, JC-1 monomers. Scale bar, 500 μ m. (B) Mitochondrial superoxide ($O_2^{\bullet-}$) generation was visualized with mtSOX Deep Red probe after 0 and 40 μ M L-OHP treatment for 2 h. Representative images of the liver organoids are shown. Red, $O_2^{\bullet-}$. BF, brightfield. Scale bar, 200 μ m. (C) Fluorescence intensity ratio (red/green) of (A). Each dot indicates an organoid. (D) Fluorescence intensity per area of (B). Each dot indicates an organoid. (E) The amount of intracellular total GSH at each time point of repeated doses administered every 24 h, extending up to either 72 h or 120 h. (F) Cytotoxicity index of liver organoid with repeated doses of 40 μ M L-OHP \pm 2 mM NAC for 72 h. These assays were performed in duplicates and representative data were shown. Bars indicate mean \pm SD. Statistical significance was determined with a two-sided Welch's *t*-test (C, D, F) or ANOVA followed by Dunnett's test (compared with *t* = 0 h) (E). **p* < 0.05, ***p* < 0.01, ****p* < 0.001, *****p* < 0.0001.



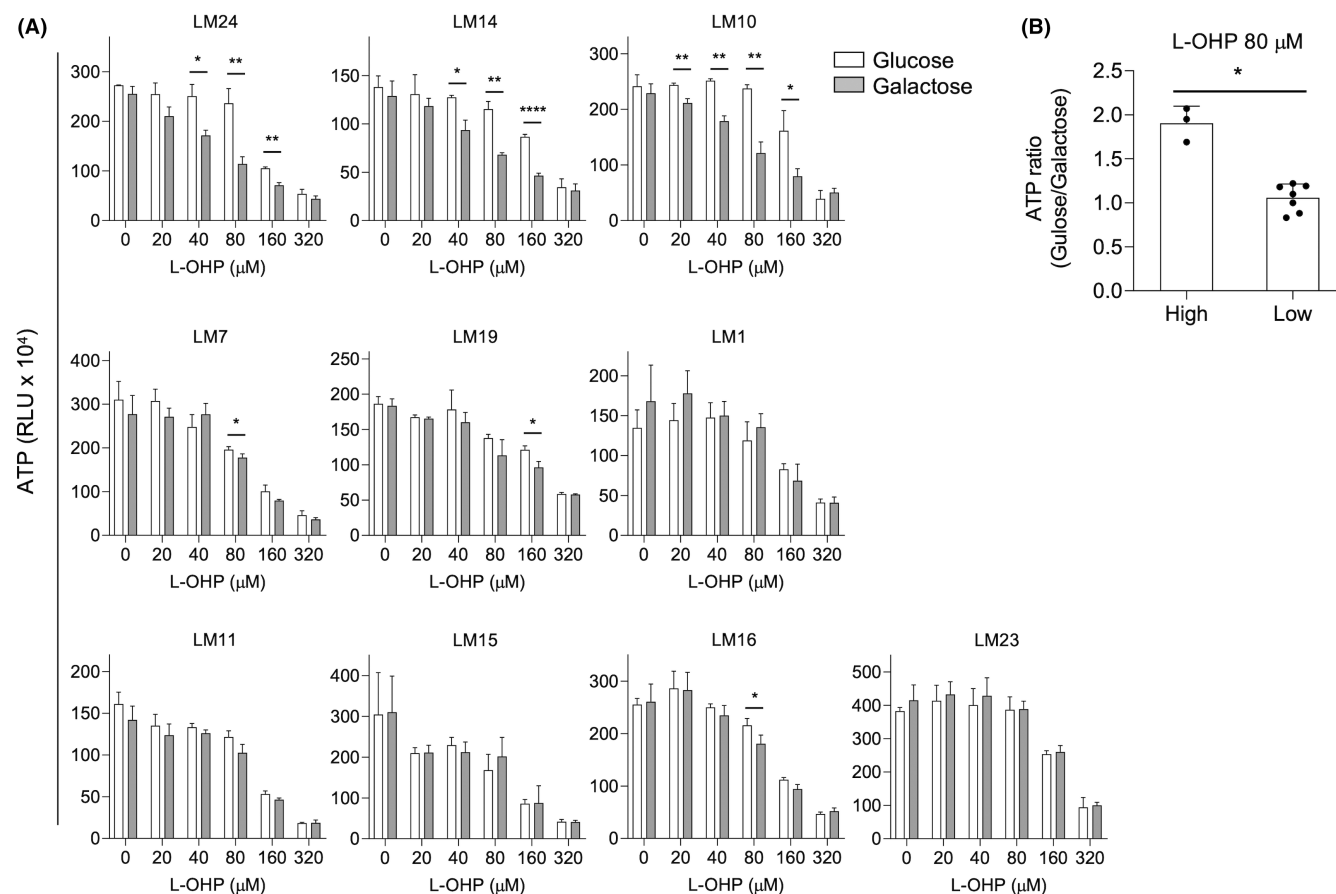


FIGURE 5 A simple test method to assess the risk of hepatic mitochondrial oxidative damage. (A) Intracellular ATP levels in liver organoids cultured in standard (glucose) or galactose differentiation medium with a single dose of L-OHP at the indicated concentrations for 72 h. (B) The ratio of intracellular ATP (glucose/galactose) in liver organoids at 80 μM L-OHP is presented in (A). Each dot indicates independent patients in the high-grade group or the low-grade group. Bars indicate mean ± SD. Statistical significance was determined with a two-sided Welch's *t*-test (A) or two-sided Mann–Whitney *U* test (B). **p* < 0.05. ***p* < 0.01. *****p* < 0.0001.

In our study, the patients categorized into the high-grade liver injury group presented clinical symptoms characteristic of L-OHP-induced liver injury with relatively mild elevations in AST and ALT, which suggests the possibility of severe L-OHP-induced liver injury.^{4,22} The patients categorized in the low-grade liver injury group appeared to have no or undetectable L-OHP-induced liver injury since they presented no clinical symptoms characteristic of L-OHP. Thus, the examination of liver organoids derived from these patients would provide us with good opportunities to examine the differences in the characteristics of patient-derived liver organoids by utilizing their clinical information.

The mechanisms underlying L-OHP-induced liver toxicity have been previously studied in animal models by multiple researchers. Robinson et al. showed a reduction in total liver GSH with FOLFOX-induced SOS and upregulation of genes implicated in oxidative stress in a mouse model.²⁸ Lin et al. and Lu et al. also studied L-OHP-induced liver toxicity using mouse models and

found increased levels of malondialdehyde and GSH or ROS and decreased levels of SOD and GSH-Px in the liver with L-OHP treatment.^{41,42} These reports demonstrated that oxidative stress plays an important role in L-OHP-induced liver toxicity in vivo. Additionally, in a study by Tabassum et al., liver mitochondria extracted from rats were utilized, revealing that treatment with L-OHP led to heightened oxidative stress markers as well as elevated mitochondrial Mn-SOD activities. Furthermore, the study observed a decrease in GSH levels, suggesting that mitochondria are susceptible targets for L-OHP-induced toxicity.²⁹ These reports collectively suggest that the toxic response to L-OHP may be caused by the oxidative stress on mitochondria.

L-OHP treatment may damage liver sinusoidal epithelial cells (LSECs) and disrupt the hepatocyte plate, resulting in sinusoidal injury and impaired hepatic circulation.^{24,28,43} Thus, in vitro assays using primary LSECs or primary hepatocytes from individual patients may provide useful information on liver toxicity if the mitochondrial

oxidative stress induced by L-OHP is properly examined. However, both primary cell types obtained from individual patients cannot be used since they already have mitochondrial membrane damage due to cryopreservation.^{44,45} In contrast, the mitochondrial membrane and functions of liver organoids were found to be preserved, as shown in our current study. And they were able to survive in a galactose medium which would force the cultured cells to shift their major source of energy production from glycolysis to mitochondrial oxidative phosphorylation. Changes in the energy metabolism of liver organoids due to different sugar sources have not been previously studied. Galactose undergoes conversion into glucose-1-phosphate through the Leloir pathway, subsequently entering both glycolysis and oxidative phosphorylation.⁴⁶ In situations where the sole sugar source is galactose, this conversion process consumes ATP, leading to a reduction in the net ATP production from glycolysis. Consequently, cells must rely more heavily on oxidative phosphorylation than glycolysis to generate the ATP required for survival.^{47–49} L-OHP-induced cytotoxicity can probably only be reliably assessable under conditions where the energy metabolism of cells resembles that of in vivo liver cells, which predominantly rely on oxidative phosphorylation for ATP production.

A novel finding in our study was the correlation observed between L-OHP-induced cytotoxicity in patient-derived liver organoids, attributed to mitochondrial oxidative damage, and the clinical severity of L-OHP-induced liver injury. The factors that modulate susceptibility to L-OHP-induced oxidative damage in the liver remain unclear. Based on our results, we discuss the possibility of these underlying factors. In our study, liver organoids derived from the high-grade group showed an obvious increase in $O_2^{\bullet-}$ levels early after L-OHP treatment. $O_2^{\bullet-}$ forms peroxynitrite ($ONOO^-$) and hydroxyl radicals ($^{\bullet}OH$), which are the most reactive oxygen species that interact with lipids, DNA, and proteins, causing the loss of mitochondrial membrane integrity.^{50,51} Therefore, enzyme activities involved in regulating $O_2^{\bullet-}$ levels and subsequent antioxidant processes may play an important role in mitochondrial oxidative stress management. For instance, genetic polymorphisms of Mn-SOD, an enzyme that eliminates $O_2^{\bullet-}$, and GSH-Px, have been reported to affect their enzymatic activities and are involved in drug-induced liver injury susceptibility.^{52,53} Intracellular concentrations of L-OHP may also vary among individuals. For instance, the glutathione-S-transferase (GST) enzyme mediates the conjugation of GSH with L-OHP, and this conjugate is subsequently excreted from the cell⁵⁴; however, it has been reported that the *GSTM1/GSTT1*-null genotype loses GST activity.⁵⁵ Organic cationic transporter 1 plays an important role in L-OHP uptake,⁵⁶ and these variants are known to reduce transport activity.⁵⁷

Further examination of these possibilities will enhance our understanding about the individual susceptibilities to L-OHP-induced liver injury.

The compounds of interest can be categorized into mitochondrial and non-mitochondrial toxicants using the assay supplied with two types of sugar, glucose, and galactose.⁵⁸ Herein, we show the usefulness of a simple and clinically applicable test method using liver organoids cultured in two types of medium and their ATP ratios to assess the risk of hepatic mitochondrial oxidative damage. Using this method, the ATP ratios in the 80 μ M L-OHP treatment were clearly different between the high- and low-grade groups. We examined liver organoids derived from resected liver tissues of patients who underwent L-OHP-based chemotherapy. While our observations revealed preserved mitochondrial membrane integrity and functions in the liver organoids across all patients, it is important to note that we cannot definitively exclude the possibility of our results being influenced by preceding mitochondrial damage caused by L-OHP. Therefore, prospective studies using liver organoids derived from chemotherapy-naïve patients are required to confirm our findings. Our results warrant further examination with a larger number of patients.

In conclusion, our results suggest that L-OHP-induced liver injury is caused by mitochondrial oxidative damage. Furthermore, we provided evidence that individual susceptibility to L-OHP-induced liver injury can be assessed using patient-derived liver organoids to provide useful information for planning chemotherapy. This in vitro test method might also be useful for predicting liver toxicities in individual patients receiving other cancer drugs that cause liver mitochondrial damage, including sorafenib and regorafenib,⁵⁹ used for hepatocellular carcinoma.

AUTHOR CONTRIBUTIONS

Kumiko Tatsumi: Conceptualization (lead); data curation (equal); formal analysis (lead); funding acquisition (supporting); investigation (lead); methodology (lead); project administration (equal); visualization (lead); writing – original draft (lead); writing – review and editing (lead). **Hiroshi Wada:** Methodology (supporting); resources (lead); writing – review and editing (equal). **Shinichiro Hasegawa:** Methodology (supporting); resources (lead); writing – review and editing (equal). **Kei Asukai:** Methodology (supporting); resources (lead); writing – review and editing (equal). **Shigenori Nagata:** Investigation (supporting); methodology (supporting); resources (lead); visualization (supporting); writing – review and editing (equal). **Tomoya Ekawa:** Formal analysis (supporting); investigation (supporting); writing – review and editing (equal). **Takashi Akazawa:** Data curation (equal); formal analysis (supporting);

investigation (supporting); writing – review and editing (equal). **Yu Mizote**: Data curation (equal); formal analysis (supporting); investigation (supporting); writing – review and editing (equal). **Shintaro Okumura**: Conceptualization (lead); methodology (lead); project administration (equal); supervision (lead); writing – original draft (lead); writing – review and editing (lead). **Ryosuke Okamura**: Conceptualization (supporting); project administration (equal); supervision (supporting); writing – original draft (supporting); writing – review and editing (equal). **Masayuki Ohue**: Resources (supporting); writing – review and editing (equal). **Kazutaka Obama**: Conceptualization (supporting); project administration (equal); supervision (lead); writing – review and editing (equal). **Hideaki Tahara**: Conceptualization (lead); funding acquisition (lead); project administration (equal); supervision (lead); writing – original draft (lead); writing – review and editing (equal).

ACKNOWLEDGMENTS

The authors thank Yachiyo Kumamoto and Satomi Yoshida for their technical support throughout this study. We also thank Dr. Seichi Ishida for valuable advice regarding the cytotoxicity assays.

FUNDING INFORMATION

This work was supported by funding from the Osaka International Cancer Institute and partly by the Project for Research on Development of New Drugs (grant number 22ak0101187h0101) from the Japan Agency for Medical Research and Development.

CONFLICT OF INTEREST STATEMENT

The authors have no conflict of interest.

DATA AVAILABILITY STATEMENT

The data that support the findings of this study are available from the corresponding author upon reasonable request.

ETHICS STATEMENT

Approval of the research protocol by an Institutional Review Board: The present study was approved by the ethics committee of the Osaka International Cancer Institute (IRB protocol number: 18231). This study was conducted in accordance with the principles of the Declaration of Helsinki.

CONSENT

Written informed consent was received from all patients.

Registry and the Registration No. of the study/trial: N/A.

Animal Studies: N/A.

ORCID

Kumiko Tatsumi  <https://orcid.org/0009-0002-9300-183X>
Takashi Akazawa  <https://orcid.org/0000-0002-4155-9228>
Yu Mizote  <https://orcid.org/0009-0006-9662-322X>
Shintaro Okumura  <https://orcid.org/0000-0002-1480-4101>

REFERENCES

1. Fakih MG. Metastatic colorectal cancer: current state and future directions. *J Clin Oncol*. 2015;33:1809-1824.
2. Adam R, Wicherts DA, de Haas RJ, et al. Patients with initially unresectable colorectal liver metastases: is there a possibility of cure? *J Clin Oncol*. 2009;27:1829-1835.
3. Nakano H, Oussoultzoglou E, Rosso E, et al. Sinusoidal injury increases morbidity after major hepatectomy in patients with colorectal liver metastases receiving preoperative chemotherapy. *Ann Surg*. 2008;247:118-124.
4. Soubrane O, Brouquet A, Zalinski S, et al. Predicting high grade lesions of sinusoidal obstruction syndrome related to oxaliplatin-based chemotherapy for colorectal liver metastases: correlation with post-hepatectomy outcome. *Ann Surg*. 2010;251:454-460.
5. Tamandl D, Klinger M, Eipeldauer S, et al. Sinusoidal obstruction syndrome impairs long-term outcome of colorectal liver metastases treated with resection after neoadjuvant chemotherapy. *Ann Surg Oncol*. 2011;18:421-430.
6. Ando Y, Saka H, Ando M, et al. Polymorphisms of UDP-glucuronosyltransferase gene and irinotecan toxicity: a pharmacogenetic analysis. *Cancer Res*. 2000;60:6921-6926.
7. Minami H, Sai K, Saeki M, et al. Irinotecan pharmacokinetics/pharmacodynamics and UGT1A genetic polymorphisms in Japanese: roles of UGT1A1*6 and *28. *Pharmacogenet Genomics*. 2007;17:497-504.
8. Innocenti F, Undevia SD, Iyer L, et al. Genetic variants in the UDP-glucuronosyltransferase 1A1 gene predict the risk of severe neutropenia of irinotecan. *J Clin Oncol*. 2004;22:1382-1388.
9. Agency EM. EMA Recommendations on DPD Testing Prior to Treatment with Fluorouracil, Capecitabine, Tegafur and Flucytosine. 2020.
10. Henricks LM, Lunenburg CATC, de Man FM, et al. DPYD genotype-guided dose individualisation of fluoropyrimidine therapy in patients with cancer: a prospective safety analysis. *Lancet Oncol*. 2018;19:1459-1467.
11. Vreuls CP, Olde Damink SW, Koek GH, et al. Glutathione S-transferase M1-null genotype as risk factor for SOS in oxaliplatin-treated patients with metastatic colorectal cancer. *Br J Cancer*. 2013;108:676-680.
12. Yu YY, Zhu YJ, Xiao ZZ, et al. The pivotal application of patient-derived organoid biobanks for personalized treatment of gastrointestinal cancers. *Biomark Res*. 2022;10:73.
13. Ganesh K, Wu C, O'Rourke KP, et al. A rectal cancer organoid platform to study individual responses to chemoradiation. *Nat Med*. 2019;25:1607-1614.
14. Mo S, Tang P, Luo W, et al. Patient-derived organoids from colorectal cancer with paired liver metastasis reveal tumor heterogeneity and predict response to chemotherapy. *Adv Sci (Weinh)*. 2022;9:e2204097.
15. Wang T, Pan W, Zheng H, et al. Accuracy of using a patient-derived tumor organoid culture model to predict the response

- to chemotherapy regimens in stage IV colorectal cancer: a blinded study. *Dis Colon Rectum*. 2021;64:833-850.
16. Huch M, Gehart H, van Boxtel R, et al. Long-term culture of genome-stable bipotent stem cells from adult human liver. *Cell*. 2015;160:299-312.
 17. Gómez-Mariano G, Matamala N, Martínez S, et al. Liver organoids reproduce alpha-1 antitrypsin deficiency-related liver disease. *Hepatol Int*. 2020;14:127-137.
 18. Brooks A, Liang X, Zhang Y, et al. Liver organoid as a 3D in vitro model for drug validation and toxicity assessment. *Pharmacol Res*. 2021;169:105608.
 19. Yu Z, Huang R, Zhao L, et al. Safety profile of oxaliplatin in 3,687 patients with cancer in China: a post-marketing surveillance study. *Front Oncol*. 2021;11:757196.
 20. Gangi A, Lu SC. Chemotherapy-associated liver injury in colorectal cancer. *Therap Adv Gastroenterol*. 2020;13:1756284820924194.
 21. National Cancer Institute. Common Terminology Criteria for Adverse Events (CTCAE). v5.0. 2017. Access February 27, 2023. https://ctep.cancer.gov/protocoldevelopment/electronic_applications/ctc.htm
 22. Nalbantoglu IL, Tan BR Jr, Linehan DC, Gao F, Brunt EM. Histological features and severity of oxaliplatin-induced liver injury and clinical associations. *J Dig Dis*. 2014;15:553-560.
 23. Overman MJ, Maru DM, Charnsangavej C, et al. Oxaliplatin-mediated increase in spleen size as a biomarker for the development of hepatic sinusoidal injury. *J Clin Oncol*. 2010;28:2549-2555.
 24. Rubbia-Brandt L, Lauwers GY, Wang H, et al. Sinusoidal obstruction syndrome and nodular regenerative hyperplasia are frequent oxaliplatin-associated liver lesions and partially prevented by bevacizumab in patients with hepatic colorectal metastasis. *Histopathology*. 2010;56:430-439.
 25. Tabernilla A, Dos Santos RB, Pieters A, et al. In vitro liver toxicity testing of chemicals: a pragmatic approach. *Int J Mol Sci*. 2021;22:5038.
 26. Riss T, Niles A, Moravec R, Karassina N, Vidugiriene J. Cytotoxicity assays: in vitro methods to measure dead cells. In: Markossian S, Grossman A, Brimacombe K, et al., eds. *Assay Guidance Manual*. Eli Lilly & Company and the National Center for Advancing Translational Sciences; 2019.
 27. Rubbia-Brandt L, Tauzin S, Brezault C, et al. Gene expression profiling provides insights into pathways of oxaliplatin-related sinusoidal obstruction syndrome in humans. *Mol Cancer Ther*. 2011;10:687-696.
 28. Robinson SM, Mann J, Vasilaki A, et al. Pathogenesis of FOLFOX induced sinusoidal obstruction syndrome in a murine chemotherapy model. *J Hepatol*. 2013;59:318-326.
 29. Tabassum H, Waseem M, Parvez S, Qureshi MI. Oxaliplatin-induced oxidative stress provokes toxicity in isolated rat liver mitochondria. *Arch Med Res*. 2015;46:597-603.
 30. Fu D, Mitra K, Sengupta P, Jarnik M, Lippincott-Schwartz J, Arias IM. Coordinated elevation of mitochondrial oxidative phosphorylation and autophagy help drive hepatocyte polarization. *Proc Natl Acad Sci U S A*. 2013;110:7288-7293.
 31. Will Y, Dykens J. Mitochondrial toxicity assessment in industry – a decade of technology development and insight. *Expert Opin Drug Metab Toxicol* 2014; 10: 1061-1067.
 32. Jastroch M, Divakaruni AS, Mookerjee S, Treberg JR, Brand MD. Mitochondrial proton and electron leaks. *Essays Biochem*. 2010;47:53-67.
 33. Palmer G, Horgan DJ, Tisdale H, Singer TP, Beinert H. Studies on the respiratory chain-linked reduced nicotinamide adenine dinucleotide dehydrogenase. XIV. Location of the sites of inhibition of rotenone, barbiturates, and piericidin by means of electron paramagnetic resonance spectroscopy. *J Biol Chem*. 1968;243:844-847.
 34. Lu SC. Glutathione synthesis. *Biochim Biophys Acta*. 2013;1830:3143-3153.
 35. Aldini G, Altomare A, Baron G, et al. N-acetylcysteine as an antioxidant and disulphide breaking agent: the reasons why. *Free Radic Res*. 2018;52:751-762.
 36. Francisqueti-Ferron FV, Ferron AJT, Garcia JL, et al. Basic concepts on the role of nuclear factor erythroid-derived 2-like 2 (Nrf2) in age-related diseases. *Int J Mol Sci*. 2019;20:3208.
 37. de Andrade KQ, Moura FA, dos Santos JM, de Araújo OR, de Farias Santos JC, Goulart MO. Oxidative stress and inflammation in hepatic diseases: therapeutic possibilities of N-acetylcysteine. *Int J Mol Sci*. 2015;16:30269-30308.
 38. Abdalla EK, Vauthey JN, Ellis LM, et al. Recurrence and outcomes following hepatic resection, radiofrequency ablation, and combined resection/ablation for colorectal liver metastases. *Ann Surg*. 2004;239:818-827; discussion 825-817.
 39. Kanemitsu Y, Shimizu Y, Mizusawa J, et al. Hepatectomy followed by mFOLFOX6 versus hepatectomy alone for liver-only metastatic colorectal cancer (JCOG0603): a phase II or III randomized controlled trial. *J Clin Oncol*. 2021;39:3789-3799.
 40. Hasegawa K, Saiura A, Takayama T, et al. Adjuvant Oral uracil-tegafur with leucovorin for colorectal cancer liver metastases: a randomized controlled trial. *PloS One*. 2016;11:e0162400.
 41. Lin Y, Li Y, Hu X, et al. The hepatoprotective role of reduced glutathione and its underlying mechanism in oxaliplatin-induced acute liver injury. *Oncol Lett*. 2018;15:2266-2272.
 42. Lu Y, Lin Y, Huang X, Wu S, Wei J, Yang C. Oxaliplatin aggravates hepatic oxidative stress, inflammation and fibrosis in a non-alcoholic fatty liver disease mouse model. *Int J Mol Med*. 2019;43:2398-2408.
 43. Ryan P, Nanji S, Pollett A, et al. Chemotherapy-induced liver injury in metastatic colorectal cancer: semiquantitative histologic analysis of 334 resected liver specimens shows that vascular injury but not steatohepatitis is associated with pre-operative chemotherapy. *Am J Surg Pathol*. 2010;34:784-791.
 44. Liu C, Sekine S, Ito K. Assessment of mitochondrial dysfunction-related, drug-induced hepatotoxicity in primary rat hepatocytes. *Toxicol Appl Pharmacol*. 2016;302:23-30.
 45. Stéphenne X, Najimi M, Ngoc DK, et al. Cryopreservation of human hepatocytes alters the mitochondrial respiratory chain complex 1. *Cell Transplant*. 2007;16:409-419.
 46. Frey PA. The Leloir pathway: a mechanistic imperative for three enzymes to change the stereochemical configuration of a single carbon in galactose. *FASEB J*. 1996;10:461-470.
 47. Rossignol R, Gilkerson R, Aggeler R, Yamagata K, Remington SJ, Capaldi RA. Energy substrate modulates mitochondrial structure and oxidative capacity in cancer cells. *Cancer Res*. 2004;64:985-993.
 48. Marroquin LD, Hynes J, Dykens JA, Jamieson JD, Will Y. Circumventing the Crabtree effect: replacing media glucose with galactose increases susceptibility of HepG2 cells to mitochondrial toxicants. *Toxicol Sci*. 2007;97:539-547.
 49. Swerdlow RH, Aires D, Lu J, et al. Glycolysis-respiration relationships in a neuroblastoma cell line. *Biochim Biophys Acta*. 2013;1830:2891-2898.

50. Juan CA, Pérez de la Lastra JM, Plou FJ, Pérez-Lebeña E. The chemistry of reactive oxygen species (ROS) revisited: outlining their role in biological macromolecules (DNA, lipids and proteins) and induced pathologies. *Int J Mol Sci*. 2021;22:4642.
51. Indo HP, Yen HC, Nakanishi I, et al. A mitochondrial superoxide theory for oxidative stress diseases and aging. *J Clin Biochem Nutr*. 2015;56:1-7.
52. Lucena MI, Garcia-Martin E, Andrade RJ, et al. Mitochondrial superoxide dismutase and glutathione peroxidase in idiosyncratic drug-induced liver injury. *Hepatology*. 2010;52:303-312.
53. Ramachandran A, Visschers RGJ, Duan L, Akakpo JY, Jaeschke H. Mitochondrial dysfunction as a mechanism of drug-induced hepatotoxicity: current understanding and future perspectives. *J Clin Transl Res*. 2018;4:75-100.
54. Kweekel DM, Gelderblom H, Guchelaar HJ. Pharmacology of oxaliplatin and the use of pharmacogenomics to individualize therapy. *Cancer Treat Rev*. 2005;31:90-105.
55. Kurose K, Sugiyama E, Saito Y. Population differences in major functional polymorphisms of pharmacokinetics/pharmacodynamics-related genes in eastern Asians and Europeans: implications in the clinical trials for novel drug development. *Drug Metab Pharmacokinet*. 2012;27:9-54.
56. Zhang S, Lovejoy KS, Shima JE, et al. Organic cation transporters are determinants of oxaliplatin cytotoxicity. *Cancer Res*. 2006;66:8847-8857.
57. Goswami S, Gong L, Giacomini K, Altman RB, Klein TE. PharmGKB summary: very important pharmacogene information for SLC22A1. *Pharmacogenet Genomics*. 2014;24:324-328.
58. Swiss R, Niles A, Cali JJ, Nadanaciva S, Will Y. Validation of a HTS-amenable assay to detect drug-induced mitochondrial toxicity in the absence and presence of cell death. *Toxicol In Vitro*. 2013;27:1789-1797.
59. Zhang J, Salminen A, Yang X, et al. Effects of 31 FDA approved small-molecule kinase inhibitors on isolated rat liver mitochondria. *Arch Toxicol*. 2017;91:2921-2938.

SUPPORTING INFORMATION

Additional supporting information can be found online in the Supporting Information section at the end of this article.

How to cite this article: Tatsumi K, Wada H, Hasegawa S, et al. Prediction for oxaliplatin-induced liver injury using patient-derived liver organoids. *Cancer Med*. 2024;13:e7042. doi:[10.1002/cam4.7042](https://doi.org/10.1002/cam4.7042)

Supporting Information

Appendix S1. Supplementary Materials and Methods

Change in spleen size

The spleen size was determined by measuring computed tomography (CT) images using Centricity Enterprise Web software (version 3.0; GE Medical Systems, USA). According to a report by Prassopoulos *et al.*,¹ the maximum width (W) of the spleen, splenic height or length (L), and thickness at the hilum (Th) were measured, and the spleen volume was calculated using the following formula:

$$\text{Spleen volume (cm}^3\text{)} = 30 + 0.58 (W \times L \times \text{Th})$$

Changes in splenic size were determined by comparing the splenic volumes before and after L-OHP-based chemotherapy.

Histopathologic examination

Archival slides stained with Victoria Blue (VB)-H&E were available for all patients. Slides for evaluation were selected from non-neoplastic liver parenchymal sites at least 20 mm from the tumor. Histological evaluation was performed by a pathologist (S.N.) who was blinded to the patient's clinical and laboratory findings. The pathological

findings of sinusoidal dilatation and, depending on severity, hepatocellular damage, centrilobular/venular fibrosis, nodular transformation, and peliosis have been reported in L-OHP-induced hepatotoxicity.²⁻⁵ Histopathological features were classified and graded according to the criteria of Rubbia-Brandt *et al.*³ Based on the criteria, sinusoidal dilation was classified into the following four grades: absent, mild (centrilobular involvement limited to one-third of the lobular area), moderate (centrilobular involvement extending in two-thirds of the lobular area), and severe (complete lobular involvement or centrilobular involvement extending to adjacent lobules with bridging congestion). Centrilobular or venular fibrosis was classified into the following three grades: absent, mild (<50% of veins and sinusoids evaluated in 20 fields at ×200 magnification), and moderate (>50% of veins and sinusoids evaluated in 20 fields at ×200 magnification). Nodular transformation was classified into the following four grades: absent, mild (focal occasionally distinct nodular hyperplasia), moderate (focal distinct nodular hyperplasia), and severe (diffuse nodular hyperplasia corresponding to nodular regenerative hyperplasia [NRH]). Steatosis was classified into the following four grades: absent, mild (steatosis in 10–30% of hepatocytes), moderate (steatosis in 30–60% of hepatocytes), and severe (steatosis in >60% of hepatocytes). Peliosis and hepatocellular damage were described as present or absent.

Establishment and maintenance of patient-derived liver organoids

Fresh tissue samples obtained as residual tissue during the surgery were minced fresh into small pieces, at less than 0.5 mm in diameter, washed three times with ice-cold wash solution (HBSS supplemented with 1% FBS and 1% penicillin/streptomycin [P/S]), and subsequently digested with 2.5 mg/mL Liberase (Merck, 05401160001) and 10 µg/mL DNase I (Merck, DN25) for 60 to 90 min at 37°C. After pipetting, the fragments were passed through a 100 µm strainer (pluriSelect Life Science) and collected. When the fragments were observed to be larger than 100 µm, they were additionally treated with 5 mL of TrypLE Express (Thermo Fisher Scientific, 12604013) containing 10 µg/mL DNase I at 37°C for 10 to 15 min. The digests were collected and centrifuged at 400×g for 5 min at 4°C. The resulting pellets were washed with 1 mL of wash solution, centrifuged at 400×g for 5 min at 4°C, suspended in Matrigel (Corning, 356231), seeded in 24-well culture plates at 30 µL each, and cultured as described by Huch *et al.*⁶ and Broutier *et al.*⁷ In brief explanation, expansion medium was Advanced DMEM/F-12 (Thermo Fisher Scientific, 12634028) supplemented with 1% P/S (Thermo Fisher Scientific, 15140122), 1% GlutaMAX (Thermo Fisher Scientific, 12604013), 10 mM HEPES (Thermo Fisher Scientific, 15630080), 1:50 B27 supplement (Thermo Fisher Scientific, 12587010) and 1:100 N2 supplement (Thermo Fisher Scientific, 17502048), 1

1 mM *N*-Acetyl-L-cysteine (NAC, FUJIFILM Wako Pure Chemical, 015-05132), 10 nM human gastrin I (Merck, G9145) and the growth factors: 50 ng/mL human EGF (Peprotech, AF-100-15), 10% (vol/vol) Rspo1-conditioned medium (homemade prepared from 3710-001-01; R&D systems), 100 ng/mL human FGF10 (Peprotech, AF-100-26), 25 ng/mL human HGF (Peprotech, 100-39), 10 mM Nicotinamide (Sigma-Aldrich, N0636), 5 μ M A83-01 (Tocris Bioscience, 2939), and 10 μ M Forskolin (FUJIFILM Wako Pure Chemical, 067-02191). For the first 3–7 days of culture, the medium was supplemented with 25 ng/mL human Noggin (Peprotech, 120-10C), 30% (v/v) Wnt3a-conditioned medium (homemade prepared from CRL-2647; ATCC), and 10 μ M Y-27632 (FUJIFILM Wako Pure Chemical, 036-24023). After 7–14 days, liver organoids were harvested and seeded for the next passage in Matrigel or Basement Membrane Extract, Type 2 (R&D Systems, 3533-010-02).

For the morphological evaluation, liver organoids were fixed in a 10% formalin neutral buffer solution (FUJIFILM Wako Pure Chemical), embedded in paraffin, and sectioned at 2 μ m for H&E staining.

Hepatocyte differentiation culture

To obtain liver organoids that differentiated into hepatocytes, established organoids were

maintained in an expansion medium supplemented with 25 ng/mL human BMP-7 (R&D Systems, 354-BP-010) for 3–5 days after the last passage and then cultured for 5–9 days in glucose-based hepatocyte differentiation medium (standard differentiation medium). To examine the effects of galactose in the culture medium, liver organoids were additionally cultured for 3 days in a galactose-based hepatocyte differentiation medium (galactose differentiation medium) or standard differentiation medium. Hepatocyte differentiation medium contains glucose-free DMEM/Ham's F-12 (Nacalai Tesque, 09893-05) supplemented with 17 mM glucose (FUJIFILM Wako Pure Chemical, 049-31165) or 17 mM galactose (Nacalai Tesque, 16511-62), 1% P/S, 10 mM HEPES, 0.5 mM sodium pyruvate solution (Merck, S8636), 400 mg/L AlbuMAX II (Thermo Fisher Scientific, 11021029), 7.5 mg/L Human transferrin (Nacalai Tesque, 34443-44), 10 mg/L human insulin (Nacalai Tesque, 12878-86), 1.52 mg/L L-Ascorbic Acid (Merck, A92902) and the supplementals described in Huch *et al.*⁶ and Broutier *et al.*⁷; 1:50 B27 supplement, 1:100 N2 supplement, 1 mM NAC, 10 nM human gastrin I, 50 ng/mL human EGF, 25 ng/mL human HGF, 100 ng/mL human FGF19 (Peprotech, 100-32), 10 μ M DAPT (Merck, D5942), 3 μ M dexamethasone (FUJIFILM Wako Pure Chemical, 041-18861), 0.5 μ M A83-01, and 25 ng/mL human BMP7.

RNA isolation and quantitative Real-time PCR (qPCR) Analysis

RNA was isolated from freshly resected liver tissue or liver organoids using the RNeasy Mini Kit (QIAGEN) or RNeasy Micro Kit (QIAGEN), respectively, according to the manufacturer's protocol. cDNA was generated using the harvested RNA as the template with Super Script IV VILO Master Mix (Thermo Fisher Scientific). For each sample, the PCR reaction mix was prepared in a total volume of 20 μ L containing 2X TaqPath qPCR Master Mix, CG (Thermo Fisher Scientific), 20X TaqMan Expression Assay probes (Thermo Fisher Scientific), and cDNA template. TaqMan Expression Assay probes used the following genes: *GAPDH* (4326317E), *ALB* (Hs00609411_m1), *CYP3A4* (Hs00604506_m1), *LGR5* (Hs00969422_m1), and *HNF4A* (Hs00230853_m1). qPCR was performed in three wells of a StepOne Real-Time PCR System (Thermo Fisher Scientific) or a QuantStudio3 Real-Time PCR System (Thermo Fisher Scientific). The results were expressed as the average fold change in gene expression calculated using the $2^{-\Delta\Delta C_t}$ method using *GAPDH* as the internal control.

Mitochondrial membrane potential assay

Differentiated liver organoids were cultured with or without L-OHP treatment to determine the mitochondrial membrane potential. For the L-OHP treatment, the culture

medium was replaced with fresh L-OHP-containing medium (NAC-free) every 24 h for up to 48 h. For the CCCP treatment, liver organoids were cultured in galactose differentiation medium (NAC-free) containing 100 μ M CCCP (abcam, ab141229) for 1.5 h. Liver organoids were collected from the embedded gel by gently pipetting up and down using ice-cold wash buffer (HBSS supplemented with 0.25% BSA and 1% P/S) and incubated at 37°C in a fully humidified 5% CO₂ atmosphere for 30 min. The mitochondrial membrane potential was determined using the JC-1 MitoMP Detection Kit (Dojindo) according to the manufacturer's protocol. Fluorescence images of liver organoids were acquired using a ZEISS LSM900 system with ZEISS ZEN3 (blue edition) software. The fluorescence intensity was measured using a BZ-X810 microscope with BZ-H4C (Keyence).

Mitochondrial oxidative stress assay

Differentiated liver organoids were collected from the embedded gel by gently pipetting up and down using ice-cold wash buffer (HBSS supplemented with 0.25% BSA and 1% P/S) and then cultured in galactose differentiation medium (NAC-free) containing L-OHP. After 2 h of culture, liver organoids were incubated at 37°C in a fully humidified 5% CO₂ atmosphere for 10 min with mtSOX Deep Red (Dojindo) 10 μ M working solution, and

the working solution was then replaced with HBSS. Bright-field and fluorescence images were acquired using a BZ-X810 microscope to identify cells emitting red fluorescence with mitochondrial superoxide ($O_2^{\bullet-}$). The cross-sectional area and fluorescence intensity were measured using the BZ-H4C application.

ATP content assay

Liver organoids were differentiated into hepatocytes in 96-well plates, as described for the LDH leakage assay. The assay was performed in triplicate. For oligomycin A treatment, liver organoids were cultured with 5 μ M oligomycin A (AdipoGen Life Sciences, AG-CN2-0517) for 2 h. For L-OHP treatment, liver organoids were cultured in a galactose differentiation medium containing L-OHP at concentrations of 0, 20, 40, 80, 160, and 320 μ M for 72 h. Intracellular ATP content was measured by luminescence using the CellTiter-Glo Luminescent Cell Viability Assay (Promega). Luminescence was measured using a Multimode Microplate Reader Infinite M200 Plex (Tecan).

Lactate production assay

Lactate production by the differentiated liver organoids was determined in triplicate. The culture medium was replaced with fresh medium and the cells were collected within 24 h

for analysis. Lactate production was determined by measuring the amount of lactate in the supernatant, using a lactate assay kit (Dojindo). Absorbance was measured at 450 nm using a Multimode Microplate Reader Infinite M200 Plex.

Glutathione (GSH) Assay

Liver organoids were differentiated and treated with L-OHP in triplicate, as described for the LDH leakage assay. Total GSH was measured using the GSH-Glo Glutathione assay (Promega). Luminescence was measured using a Multimode Microplate Reader Infinite M200 Plex.

References

- 1 Prassopoulos P, Daskalogiannaki M, Raissaki M, Hatjidakis A, Gourtsoyiannis N. Determination of normal splenic volume on computed tomography in relation to age, gender and body habitus. *Eur Radiol.* 1997; 7: 246-248.
- 2 Rubbia-Brandt L, Audard V, Sartoretti P, et al. Severe hepatic sinusoidal obstruction associated with oxaliplatin-based chemotherapy in patients with metastatic colorectal cancer. *Ann Oncol.* 2004; 15: 460-466.
- 3 Rubbia-Brandt L, Lauwers GY, Wang H, et al. Sinusoidal obstruction syndrome and nodular regenerative hyperplasia are frequent oxaliplatin-associated liver lesions and partially prevented by bevacizumab in patients with hepatic colorectal metastasis. *Histopathology.* 2010; 56: 430-439.
- 4 Ryan P, Nanji S, Pollett A, et al. Chemotherapy-induced liver injury in metastatic colorectal cancer: semiquantitative histologic analysis of 334 resected liver specimens shows that vascular injury but not steatohepatitis is associated with preoperative chemotherapy. *Am J Surg Pathol.* 2010; 34: 784-791.

- 1 5 Nalbantoglu IL, Tan BR, Jr., Linehan DC, Gao F, Brunt EM. Histological features
2 and severity of oxaliplatin-induced liver injury and clinical associations. *J Dig Dis*.
3 2014; 15: 553-560.
- 4 6 Huch M, Gehart H, van Boxtel R, et al. Long-term culture of genome-stable
5 bipotent stem cells from adult human liver. *Cell*. 2015; 160: 299-312.
- 6 7 Broutier L, Andersson-Rolf A, Hindley CJ, et al. Culture and establishment of
7 self-renewing human and mouse adult liver and pancreas 3D organoids and their
8 genetic manipulation. *Nat Protoc*. 2016; 11: 1724-1743.
- 9

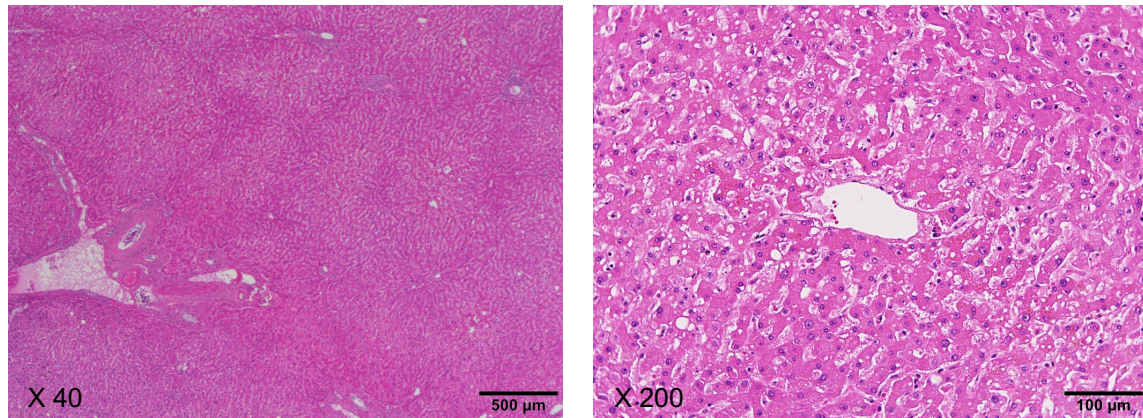


Figure S1. Histology of liver tissue of LM23 in the low-grade liver injury group.

Representative Victoria Blue (VB)-H&E staining images of non-cancerous liver tissue treated with L-OHP-based chemotherapy. A low-power field is shown in the left panel. A high-power field is shown in the right panel.

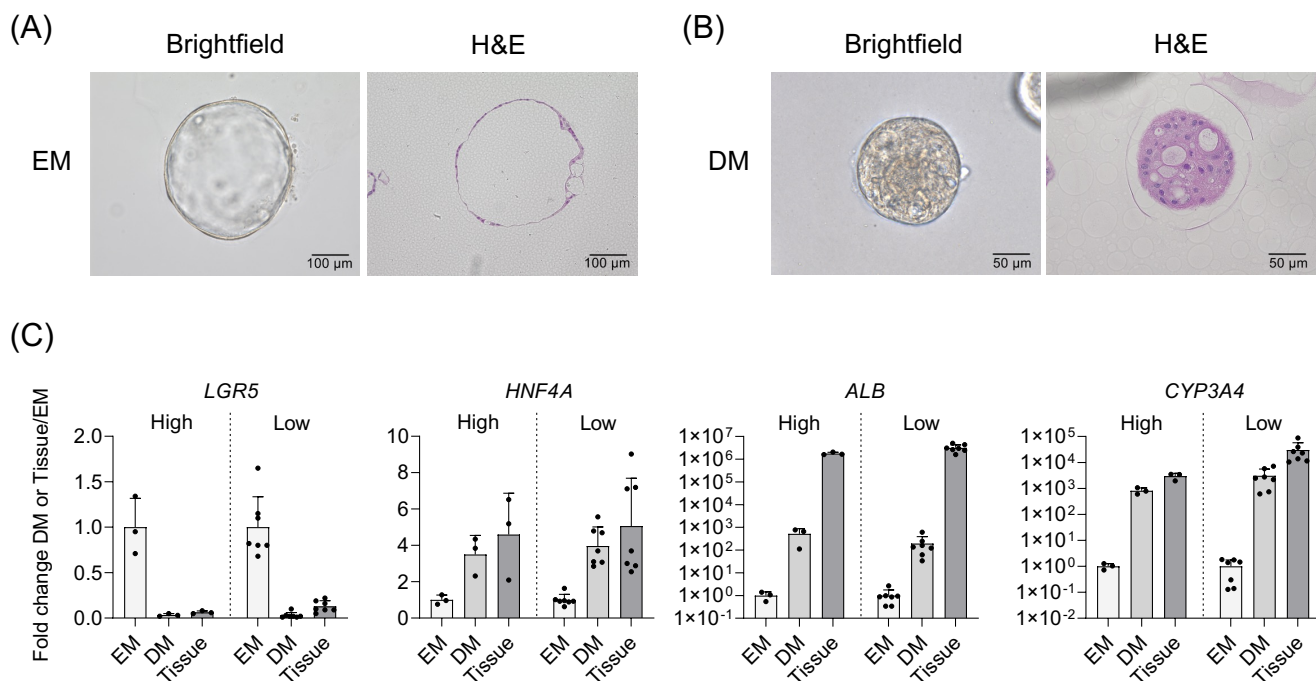


Figure S2. Characterization of liver organoids established from non-cancerous liver tissues.

(A, B) Representative bright-field and H&E staining images of a liver organoid cultured in expansion medium (EM) (A) and in differentiation medium (DM) (B). (C) Fold changes in the expression levels of the indicated genes in liver organoids cultured in conditioned media (EM and DM) and in non-cancerous liver tissues (Tissue). Each dot indicates independent patients in the high- or low-grade groups. Bars indicate mean \pm SD.

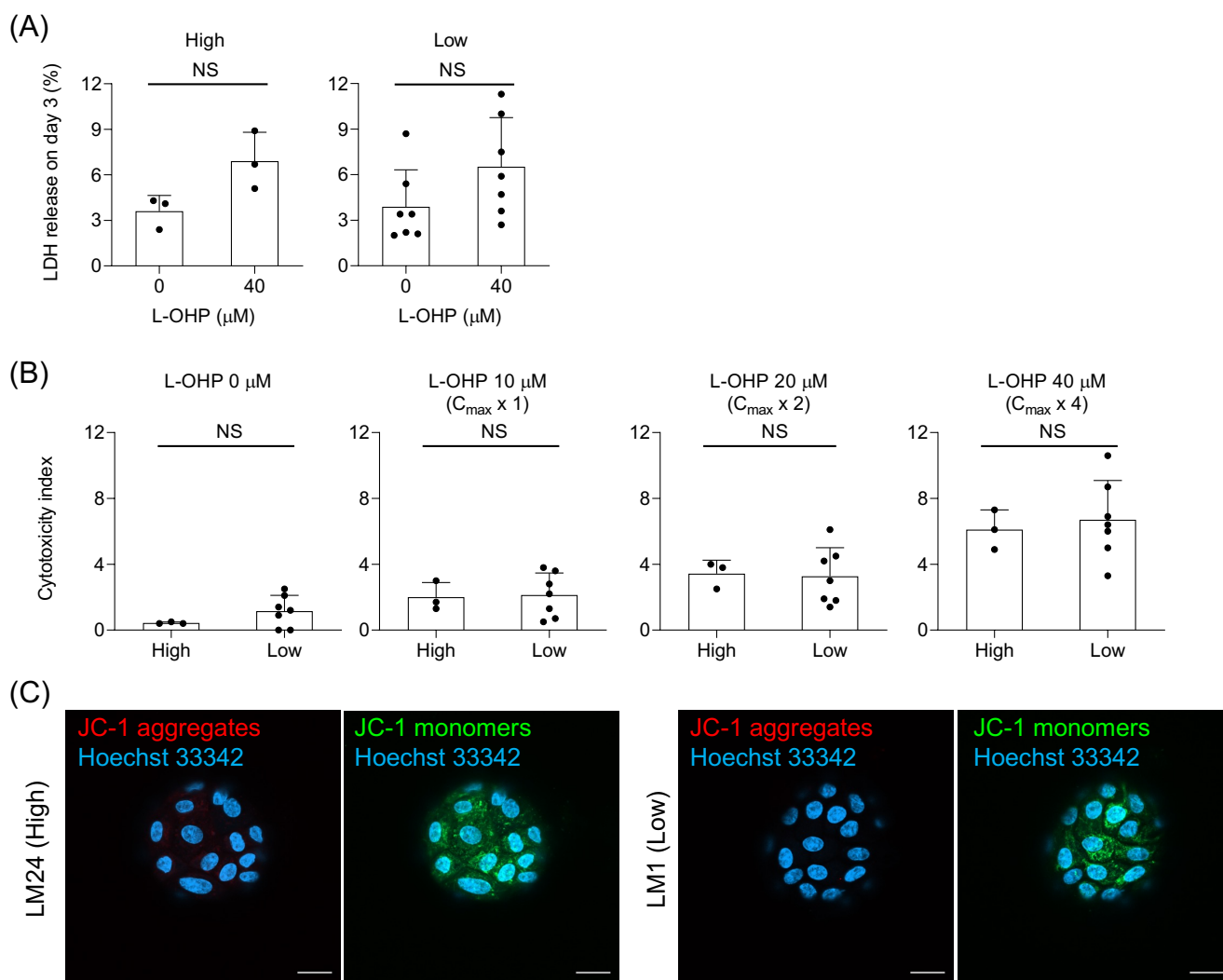


Figure S3. Assessment of cytotoxicity in liver organoids cultured in standard differentiation medium.

(A-C) Liver organoids were cultured in a standard differentiation medium for 8–11 days. (A) LDH release from liver organoids on day 3 of repeated doses of L-OHP. (B) Cytotoxicity index of liver organoids treated with repeated doses of L-OHP at the indicated concentrations for 72 h. (C) Mitochondrial condition was evaluated with a JC-1 probe. Representative images of JC-1-stained liver organoids are shown. Red, JC-1 aggregates; green, JC-1 monomers; blue, Hoechst 33342 (nuclei). Scale bar, 20 μm. For all bar graphs, each dot indicates independent patients in the high- or low-grade groups. Bars indicate mean \pm SD. Statistical significance was determined with a two-sided Welch's *t*-test (A) or two-sided Mann–Whitney *U* test (B). NS, Not Significant.

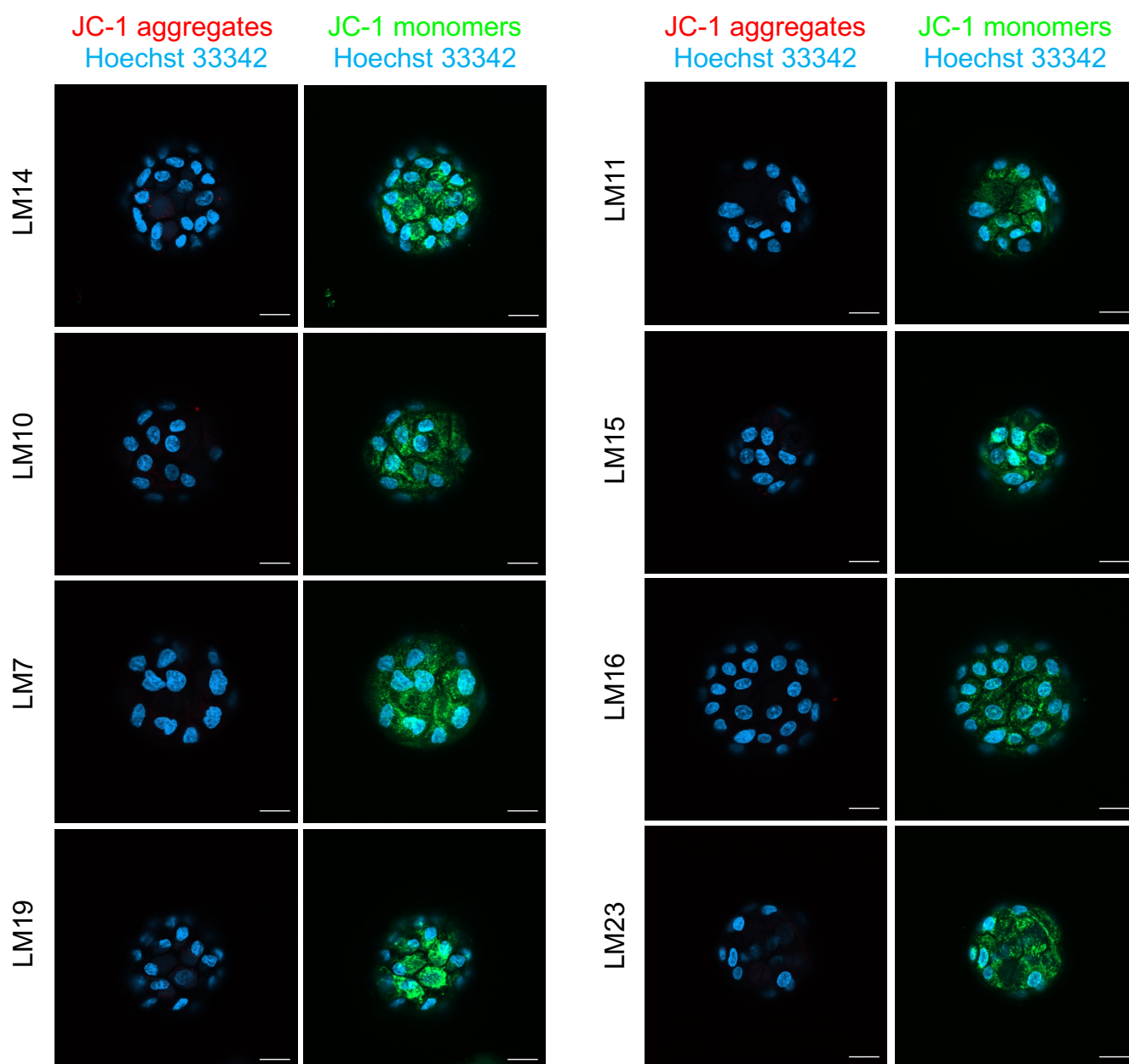


Figure S4. Representative images of JC-1-stained liver organoids cultured in standard differentiation medium.

The mitochondrial condition of liver organoids from each patient was evaluated using a JC-1 probe. Representative images of the JC-1-stained liver organoids. Red, JC-1 aggregates; green, JC-1 monomers; blue, Hoechst 33342 (nuclei). Scale bar, 20 μ m.

Supplementary Table S1 Histopathological findings of liver tissues of the patients

	High-grade group			Low-grade group						
	LM24	LM14	LM10	LM7	LM19	LM1	LM11	LM15	LM16	LM23
Sinusoidal dilatation	Mild	Moderate to severe	Moderate	Mild	Mild	Absent	Moderate	Absent	Moderate	Absent
Centrilobular/venular fibrosis	Mild	Absent	Mild	Absent	Mild	Absent	Absent	Absent	Mild	Absent
Nodular transformation	Mild	Mild	Moderate	Absent	Absent	Absent	Mild	Absent	Mild	Absent
Peliosis	Absent	Absent	Absent	Absent	Absent	Absent	Absent	Absent	Absent	Absent
Hepatocellular damage	Present	Present	Present	Absent	Absent	Absent	Absent	Absent	Absent	Absent
Steatosis	Absent	Absent	Moderate	Mild	Moderate	Mild	Absent	Mild	Severe	Absent